Voltage Driven coils within a Discrete Geometric Approach to 3D eddy-currents

R. Specogna, F. Trevisan
Università di Udine, Via delle Scienze 208, I-33100 Udine, Italy
E-mail: r.specogna@nettuno.it, trevisan@uniud.it

***Abstract*: We propose a method to account for voltage driven coils when solving 3D eddy-current problems with a discrete geometric approach. The formulation we use is based on the circulation A of the magnetic vector potential on primal edges and on a gauge function χ on conductor primal nodes. An iterative technique to make the right-hand-side term of the linear system consistent is shown. It can be used both for simple coil geometries, where the external electric field is known in advance, and in the case of more general coil geometries, provided that a steady-state current conduction problem is solved first, from the impressed voltage, using a discrete approach. The results are compared with those obtained with Finite Elements.**

***Keywords*: Eddy-currents, voltage driven coils, discrete approaches.**

I. Introduction

The modelling of voltage driven coils as sources in eddy-current problems is well known and efficient solutions are proposed in [1], [2], [3] in the framework of Finite Elements formulations. Aim of this paper is to focus on discrete geometric approaches and to introduce the algebraic equations of voltage driven coils within an existing algebraic formulation for eddy-currents [4], which "naturally" treats current driven coils. This formulation is based on the circulation of magnetic vector potential on primal edges and on a gauge function on primal nodes of a mesh made of a pair of interlocked cell complexes. We will concentrate on the computation of the array of impressed $e.m.f.$s along primal edges of coil's submesh, both for particular geometries of the coils and for more general geometries. In this last case we will solve, as first, a steady-state current conduction problem formulated in a discrete way. In both the cases we will show an iterative method that makes the right hand side of the linear system consistent so that gauging can be avoided.

II. $A-\chi$ formulation for voltage driven coils

The domain of interest D of the eddy-current problem, can be partitioned respectively into a source region D_s consisting of a voltage driven coil, a passive conductive region D_c and an air region D_a which is the complement of D_c and D_s in D. We introduce in D a pair of interlocked cell complexes [5], [6], [7]. The primal complex is simplicial with *inner* oriented cells (nodes n, edges e, faces f, cells v) and the dual complex is barycentric, with *outer* oriented cells (dual cells $\tilde{v}$, dual faces $\tilde{f}$, dual edges $\tilde{e}$, dual nodes $\tilde{n}$). The interconnections between cells of the primal or of the dual complex, are defined by the usual connectivity matrices ($\mathbf{G}$, $\mathbf{C}$, $\mathbf{D}$ and $\tilde{\mathbf{D}} = -\mathbf{G}^T$, $\tilde{\mathbf{C}} = \mathbf{C}^T$, $\tilde{\mathbf{G}} = \mathbf{D}^T$). With respect to these cell complexes, we recall the basic algebraic equations governing an eddy-current problem

$$\begin{array}{llll} \mathbf{D\Phi} = \mathbf{0} & (a), & \tilde{\mathbf{C}}\mathbf{F} = \mathbf{I} & (c) \\ \mathbf{CU} = -d_t\mathbf{\Phi} & (b), & \tilde{\mathbf{D}}\mathbf{I} = \mathbf{0} & (d), \end{array} \tag{1}$$

where (a) is *Gauss's* law relating the array of fluxes $\mathbf{\Phi}$ associated with primal faces, (b) is *Faraday's* law relating the array $\mathbf{U}$ of *e.m.f.* along primal edges, (c) is *Ampère's* law relating the array $\mathbf{F}$ of magnetic voltages associated with dual edges and the array $\mathbf{I}$ of currents crossing dual faces, (d) is *continuity* law. To these laws, discrete constitutive laws have to be considered in addition

$$\mathbf{F} = \boldsymbol{\nu}\,\mathbf{\Phi}, \qquad \mathbf{I} = \boldsymbol{\sigma}\,(\mathbf{U} + \mathbf{U}^{ext}), \tag{2}$$

where $\boldsymbol{\nu}$ (of dimension $F \times F$) and $\boldsymbol{\sigma}$ (of dimension $E \times E$) are some square mesh- and medium-dependent matrices that require *metric* notions, *material* properties and some hypothesis on the *fields* in order to be computed. The magnetic matrix $\boldsymbol{\nu}$ can be computed as described in [8], while Ohm's matrix $\boldsymbol{\sigma}$ can be computed as proposed in [4]; it is non symmetric and differs from the one used in finite elements, [1]. Finally, we indicate with $\mathbf{U}^{ext}$ the array of impressed *e.m.f.*s at primal edges of D_s.

Considering the array $\mathbf{A}'$ of circulations of the magnetic vector potential relative to primal edges e, decomposed into the closed part and its complement respectively $\mathbf{A}' = \mathbf{G}\,\boldsymbol{\chi} + \mathbf{A}$, where $\boldsymbol{\chi}$ is the array of gauge function χ associated to primal nodes [4], we can rewrite (1) combined with (2), obtaining the following equations in the frequency domain ($d_t \to i\omega$),

$$\begin{array}{ll} \tilde{\mathbf{C}}\boldsymbol{\nu}\mathbf{C}\mathbf{A} = 0 & edges \in D_a \\ (\tilde{\mathbf{C}}\boldsymbol{\nu}\mathbf{C} + i\omega\boldsymbol{\sigma})\mathbf{A} + \boldsymbol{\sigma}\mathbf{G}\boldsymbol{\chi} = \sigma\mathbf{U}^{ext} & edges \in D_s \\ (\tilde{\mathbf{C}}\boldsymbol{\nu}\mathbf{C} + i\omega\boldsymbol{\sigma})\mathbf{A} + \boldsymbol{\sigma}\mathbf{G}\boldsymbol{\chi} = 0 & edges \in D_c \\ i\omega\tilde{\mathbf{D}}\boldsymbol{\sigma}\mathbf{A} + i\omega\tilde{\mathbf{D}}\boldsymbol{\sigma}\mathbf{G}\boldsymbol{\chi} = 0 & nodes \in D_c \\ i\omega\tilde{\mathbf{D}}\boldsymbol{\sigma}\mathbf{A} + i\omega\tilde{\mathbf{D}}\boldsymbol{\sigma}\mathbf{G}\boldsymbol{\chi} = \tilde{\mathbf{D}}\boldsymbol{\sigma}\mathbf{U}^{ext} & nodes \in D_s. \end{array} \tag{3}$$

In the following we will focus on the construction of the right-hand side of the system (3) and we will derive an array of currents $\mathbf{I}^{ext}$ such that

$$\mathbf{I}^{ext} = \boldsymbol{\sigma}\mathbf{U}^{ext} \tag{4}$$

which complies with continuity law (1d).

In the case of simple geometries of D_s, such as the circular coil in Figure 1, the electric field $\mathrm{E}^{ext}(P)$ at a point $P \in D_s$ is $\mathrm{E}^{ext}(P) = U^l/(2\pi r)\hat{\phi}$, where U^l is the voltage at coil leads, $\hat{\phi}$ is the azimuthal unit vector of a cylindrical reference frame with z axis coincident with the coil axis and origin at the coil center, r is the radial coordinate of P. This way external *e.m.f.* $U_e^{ext} = \int_e \mathrm{E}^{ext} \cdot d\mathrm{l}$ along edge e

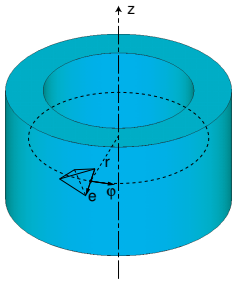

Figure 1. Geometry of source region D_s in the case of a circular coil.

can be approximated as $U_e^{ext} \approx \mathrm{E}^{ext}(g) \cdot \mathrm{e}$, where g is the barycenter of e and e is the edge vector associated with e. However, $\mathbf{I}^{ext}$ in (4), corresponding to $\mathbf{U}^{ext}$ thus obtained, does not comply with $(1d)$. Thanks to the duality between the pair of cell complexes, we have the correspondences

$$\tilde{f} \leftrightarrow e, \qquad \tilde{v} \leftrightarrow n. \tag{5}$$

Therefore to assure that for each $\tilde{v}$

$$\tilde{\mathbf{D}}\mathbf{I}^{ext} = 0 \tag{6}$$

holds, we can find a tree and the corresponding cotree subgraphs in the graph formed by coil's primal edges e and nodes n. We use currents I^{ext} associated with the cotree edges, in order to recompute the currents associated with the edges of the tree to comply with (6). To set up the algorithm we consider

- as known and fixed the currents in the array $\mathbf{I}^{ext}$ associated with dual faces crossed by a cotree edge;
- a list of all nodes in D_s.

The algorithm proceed cycling the list of nodes, until the list is empty.

Algorithm:

- For every node, find the star of edges around it.
- If all the edges of the cluster but one are marked with known current, then the current on the remaining free edge can be calculated from (6).
- The edge is marked with known current and the node is removed from the list.

The algorithm converges in a few iterations and the computing time is negligible. This way we determine a new set of currents complying with (6) and the right hand-side of (3) becomes consistent.

III. Coils of generic geometry

For a more complicated coil geometry, the impressed electric filed E^{ext} in D_s is not known in advance. Therefore we may solve, as first, a steady-state conduction current problem in a subdomain $D_s' \subset D_s$ with assigned boundary conditions. For example we focus on the circular coil geometry shown in Figure 1. To impose the boundary conditions, we can make a thick cut in D_s by introducing a slice of air and we assign the boundary conditions on the two surfaces S_1, S_2 between the thick cut and the conductor. We may assign to nodes on S_1 a null potential while to nodes on S_2 a potential equal to U^l. Thinking to a limit process, we can make the thick cut thinner and thinner until S_1 and S_2 coincide with a single cut surface S (Figure 2, on the left). This way, we avoid the thick cut and the corresponding mesh in the slice of air. We will indicate with D_s' the domain D_s with in addition the cut surface S. The labels of nodes and edges laying on the cut surface S are duplicated (in Figure 2, on the right, nodes like n and edges like e). For example, refer to the simplified 2D view of Figure 3, where a node n on S is identified by two distinct labels n_a, n_b indicating topologically two different nodes but with the same coordinates, similarly for edges like e on S. To account for this, we have to write a new incidence matrix $\mathbf{G}'$ between edges and nodes only within domain D_s'. Finally, matrix $\tilde{\mathbf{D}}'\boldsymbol{\sigma}'\mathbf{G}'$ is assembled accounting for duplicated nodes and edges. Boundary condition may be imposed by assigning potential U^l on one set of nodes lying on S (like n_a) and 0 on the other set (like n_b).

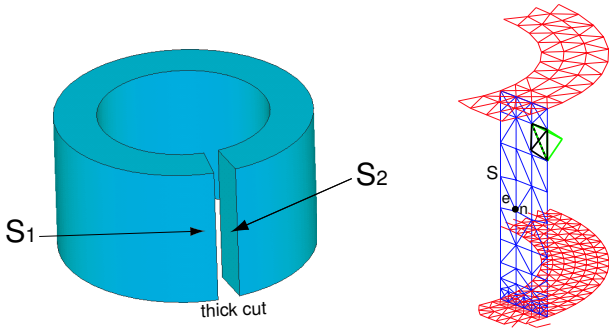

Figure 2. On the left the coil with the air cut are shown, together with the pair of surfaces S_1, S_2 between the thick cut and the conductor. On the right nodes like n and edges like e laying on S have duplicated labels.

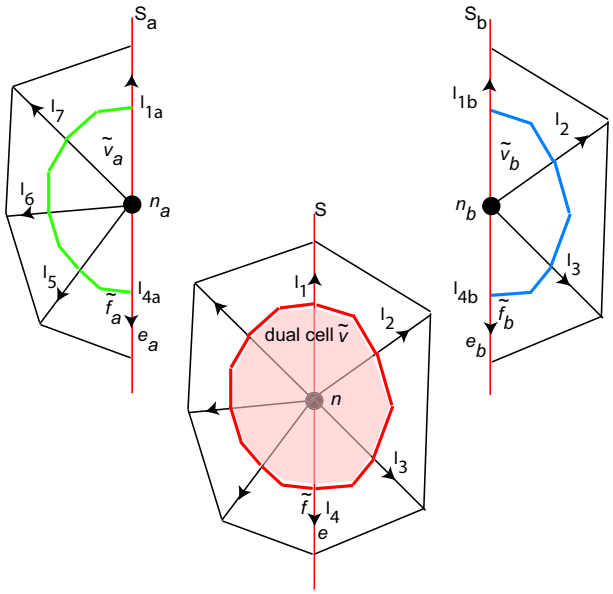

Figure 3. Schematic 2D view of a dual cell $\tilde{v}$ divided in two subcells $\tilde{v}_a$ and $\tilde{v}_b$.

To derive algebraic equations governing the steady-state conduction current problem in D_s', we substitute in $(1d)$ Ohm's constitutive law (2) written as $\mathbf{I}'^{ext} = \boldsymbol{\sigma}'\mathbf{U}'^{ext}$, where $\boldsymbol{\sigma}'$ is Ohm's constitutive matrix in D_s'. Thanks to $(1b)$ written for steady-state fields, we have $\mathbf{U}'^{ext} = -\mathbf{G}'\,\mathbf{V}'^{ext}$, where $\mathbf{V}'^{ext}$ is the array of electric scalar potentials associated to primal nodes in D_s'. We obtain the

following algebraic equations in D'_s

$$\tilde{\mathbf{D}}'\boldsymbol{\sigma}'\mathbf{G}'\mathbf{V}'^{ext} = 0, \tag{7}$$

where it can be proved that stiffness matrix $\tilde{\mathbf{D}}'\boldsymbol{\sigma}'\mathbf{G}'$ is symmetric even though $\boldsymbol{\sigma}'$ is not. We solve (7) and we can easily derive impressed voltages $\mathbf{U}'^{ext} = \mathbf{G}'\mathbf{V}'^{ext}$ for each edge of D'_s, together with currents $\mathbf{I}'^{ext} = \boldsymbol{\sigma}'\mathbf{U}'^{ext}$ for each dual face of D'_s.

We consider now dual faces like $\tilde{f}_a$ and $\tilde{f}_b$, Figure 3, which are one-to-one with edges e_a and e_b respectively laying on S. These dual faces do have non zero currents across (like I_{1a} or I_{4b} in Figure 3), even though the corresponding primal edges e_a, e_b respectively, have null voltage, each edge being on equipotential surfaces S_a and S_b respectively. These currents are not zero because the constitutive matrix $\boldsymbol{\sigma}'$ we use is not diagonal, thus the current on one dual face depends on the voltages of all the edges of the cluster of tetrahedra (on the left or on the right of S) around nodes like n_a or n_b. In general, the primal mesh is not symmetric with respect to surface S. Thence, considering dual cells like $\tilde{v}_a$ or $\tilde{v}_b$ divided by S, it happens that algebraic sum of currents crossing dual faces bounding $\tilde{v}_a$ or $\tilde{v}_b$ respectively, do not match. For example, with the notation of Figure 3, we have $I_{n_a} \neq I_{n_b}$, where $I_{n_a} = I_{4a} + I_5 + I_6 + I_{1a}$ and $I_{n_b} = I_{1b} + I_2 + I_3 + I_{4b}$. This mismatch is local, at level of the two halves of a dual cell divided by S, while globally the net current crossing S_a coincides with net current crossing S_b and we have $\sum_{n\in S} I_{n_a} = \sum_{n\in S} I_{n_b}$.

We focus now on the computation of $\mathbf{I}^{ext}$ as in (4) with respect to D_s, from the knowledge of $\mathbf{I}'^{ext}$ with respect to D'_s. To this aim we have to glue together the pair of dual cells like $\tilde{v}_a$ and $\tilde{v}_b$, obtaining dual cell $\tilde{v}$ one-to-one with primal node $n \in S$. This way, currents crossing dual faces like $f_1 = f_{1a} \bigcup f_{1b}$ in Figure 3 are the sum of currents crossing dual faces like f_{1a} and f_{1b} respectively (for example $I_1 = I_{1a} + I_{1b}$). However for any dual cell like $\tilde{v}$, continuity law (1d) is not satisfied, due to the local mismatch of net currents like I_{n_a} and I_{n_b}. This causes $\tilde{\mathbf{D}}\mathbf{I}^{ext} \neq 0$ for the subset of nodes (one-to-one with dual cells) lying on the cutting plane S. Therefore we can't use the ungauged formulation and we have to resort to the tree-cotree decomposition gauging technique increasing considerably the time required to solve (3).

To make $\mathbf{I}^{ext}$ solenoidal according to (6) we can apply the same idea at the base of the iterative algorithm described in the previous section. To this aim we find a tree and the cotree subgraphs of the graph formed by nodes and edges in D_s and we regard as free the currents associated with dual faces crossed by a tree edge. During the first iteration of the algorithm, only the subset of nodes laying on S need to be processed, because we have, by construction, that $\tilde{\mathbf{D}}\mathbf{I}^{ext} = 0$ for all the nodes in D_s except those in S.

IV. Numerical results

A. Circular coil

As reference test problem we will consider the geometry shown in Figure 4. It consist of a circular coil (10 mm of height, 12 mm of inner diameter, 18 mm of outer diameter) placed above an aluminium plate (4 mm of thickness). The coil is feeded with a sinusoidal voltage at leads $U^l = 100\,V$ with a frequency $f = 5000\,Hz$. We discretize the domain with a primal mesh having the characteristics shown in Table I. We solved the test problem using the discrete geometric approach, considering the developed methods for both particular and general geometries of the source region. For comparison, we also considered the results from a 2D Finite Elements analysis obtained using the ANSYS Finite Elements code. Absolute values of real and imaginary parts of the eddy-current density vector sampled along two lines l_1 and l_2 (l_1: length $20\,mm$, $0.4\,mm$ below conductor's surface, l_2: length $3\,mm$, at half height of the coil, Figure 4) are shown in Figures 5, 6, 7 and 8 respectively. Because the right-hand-side of the system is consistent we avoided gauging. We performed a further analysis, using the array of currents $\mathbf{I}^{ext}$ that do not comply with (6), i.e. before the application of the proposed algorithm. In this case the tree-cotree gauging technique is needed to solve the system. In table II the timing of the simulations on a portable PENTIUM IV 1.9GHz, 512MB of RAM are shown; T_t indicates the total time needed to obtain the solution, T_s is the time interval necessary to solve the linear system with a CGS solver from NAG library. The first row of Table II refers to the particular method for circular coils, the second row refers to the general method for generic coil geometries, last row shows the case where gauging is needed. All the three simulations are in very good agreement with the results from the 2D simulation obtained with Finite Elements.

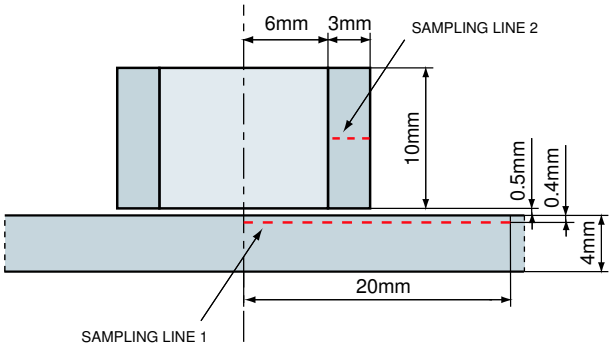

Figure 4: Geometry of the test problem.

TABLE I: Mesh data used for the benchmark

Nodes	14011
Edges	96811
Primal cells	82369
DoFs	104791
Conductor cells	28.8%
Coil cells	16.5%

TABLE II: Timing of execution

	$T_t\,[s]$	$T_s\,[s]$	ITN	$RNORM$
1	6 : 40	1 : 28	163	$9.60\,10^{-6}$
2	8 : 03	1 : 35	173	$1.65\,10^{-5}$
3	30 : 33	23 : 32	3749	$1.59\,10^{-4}$

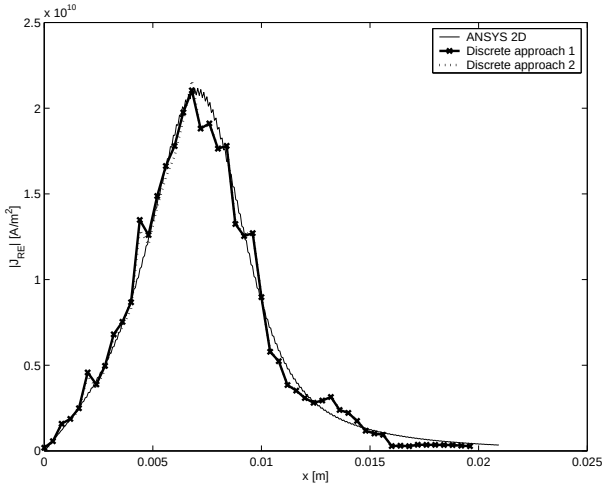

Figure 5. The absolute values of the real part of current density along l_1.

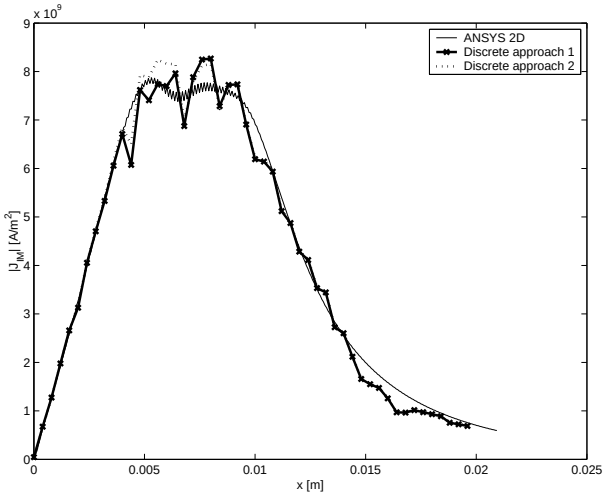

Figure 6. The absolute values of the imaginary part of current density along l_1.

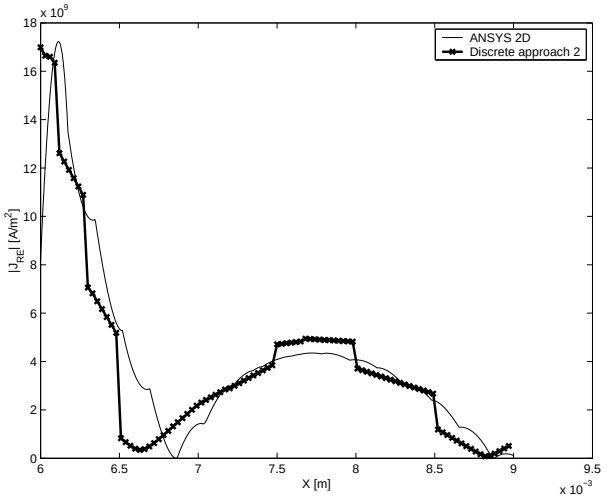

Figure 7. The absolute values of the real part of current density along l_2.

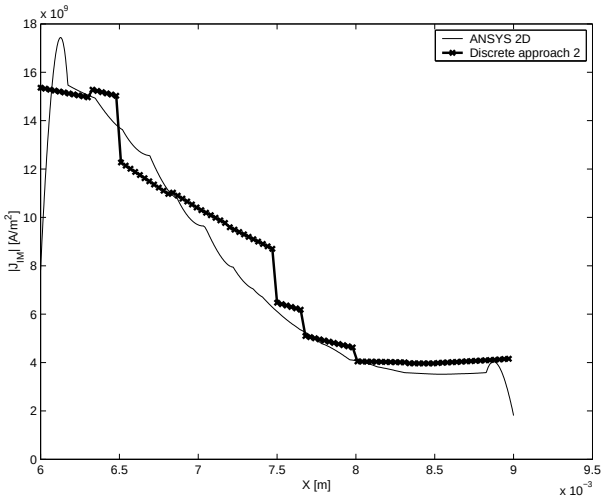

Figure 8. The absolute values of the imaginary part of current density along l_2.

B. Racetrack shaped coil

As second and more general benchmark, we use the geometry of the TEAM Workshop problem 7 (see Figure 9). It consists of a racetrack shaped coil (square coil with 200 mm of width, 100 mm of height, 50/25 mm of maximum/minimum radius at the corner) driven by a time harmonic voltage (amplitude $U^l = 100V$, frequency $f = 200Hz$) over an asymmetrical conductor (a square plate of 294 mm of width and 19 mm of thickness) with a hole (108 mm x 108 mm). Both the conductivities of the conductor and of the coil are $\sigma_C = \sigma_S = 4 \cdot 10^7\, S/m$. We discretize the domain with a primal mesh having the characteristics shown in Table III. We solved the test problem using the developed approach for generic coil geometry. The total execution time is 25:33 min while 5:21 min are needed to solve the linear system (224 iterations, $3.60 \cdot 10^{-4}$ of normalized residual). Less then 4 seconds are necessary to solve (7) and to determine the discrete divergence free array $\mathbf{I}^{ext}$ according to the proposed algorithm. The induced current density in the conductor (drawn in Figure 10) is sampled over a line (just under the cutting plane, length 294 mm, 1 mm below conductor's surface, Figure 9). In the Figures 11 and 12 we plot the absolute values of the real and imaginary parts respectively of induced current density along the sampling line.

TABLE III: MESH DATA USED FOR THE SECOND BENCHMARK

Nodes	24141
Edges	166293
Primal cells	142125
DoFs	176260
Conductor cells	23%
Coil cells	7%

V. CONCLUSION

We have presented a possible approach to treat voltage driven coils with simple geometries, in eddy-current problems within a geometric $a-\chi$ formulation. For more complicated geometries a steady-state current conduction problem is solved with a discrete geometric approach. An algorithm to make the right hand side of the final linear system consistent is also proposed. The presented methods are tested against a reference problem. The results obtained

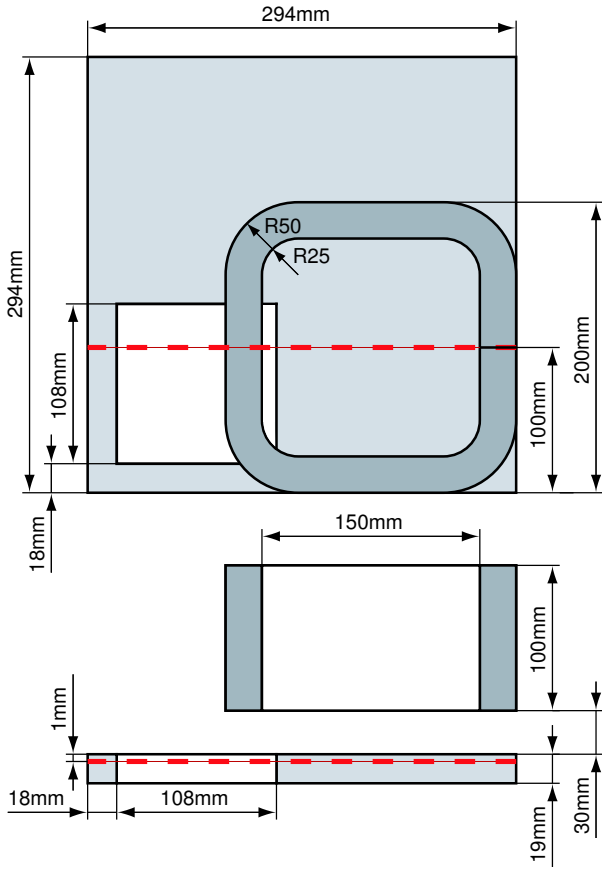

Figure 9. The TEAM problem 7 geometry is used as second benchmark.

are in a very good agreement to each others and with the results from a 2D Finite Element code. Finally the geometry of a race-track coil above a conducting plate (TEAM Workshop problem 7) is analyzed with the proposed approach.

REFERENCES

[1] O. Biro, K. Preis, "On the Use of the Magnetic Vector Potential in the Finite Element Analysis of Three-Dimensional Eddy Currents", IEEE Trans. Mag. Vol. 25, No. 4, 1989.

[2] O. Biro, K. Preis, W. Renhart, G. Vrisk and K.R. Richter, "Computation of 3D current driven skin effect problems using a current vector potential", IEEE Transactions on Magnetics, vol. 29, pp. 1325-1328, March 1993.

[3] O. Biro, K. Preis, G. Buchgraber, I. Tičar, "Voltage-Driven Coils in Finite-Element Formulations Using a Current Vector and Magnetic Scalar Potential", IEEE Transactions on Magnetics, vol. 40, pp. 1286-1289, March 2004.

[4] F. Trevisan, "3-D Eddy Current Analysis With the Cell Method for NDE Problems", IEEE Trans., MAG-40, No. 2, March 2004, pp. 1314-1317.

[5] E. Tonti, "Finite Formulation of the Electromagnetic Field", IEEE Trans. on Mag. Vol. 38, No. 2, 2002, pp. 333-336.

[6] A. Bossavit, "How weak is the Weak Solution in finite elements methods?", IEEE Trans. Mag. Vol 34, No. 5, 1998, pp. 2429-2432.

[7] A. Bossavit, L. Kettunen "Yee-like Schemes on Staggered Cellular Grids: A synthesis Between FIT and FEM Approaches", Vol. 36, No. 4, July 2000.

[8] F. Trevisan, L. Kettunen, "Geometric interpretation of discrete approaches to solving Magnetostatics", Vol. 40, No. 2, March 2004, pp. 361-365.

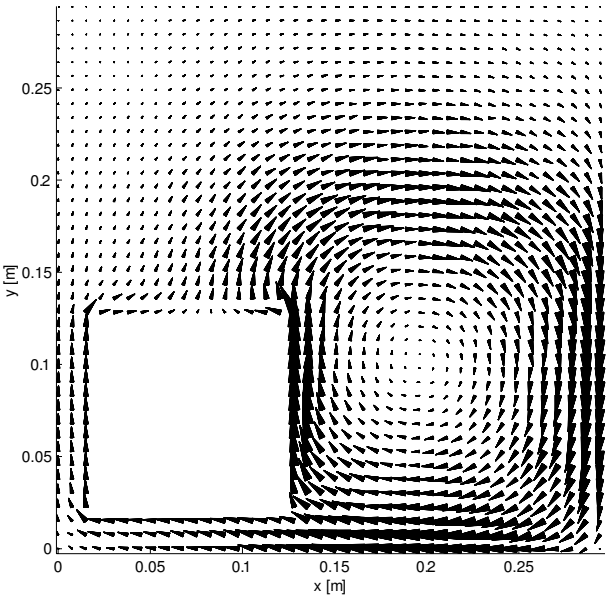

Figure 10: The induced current in the plate.

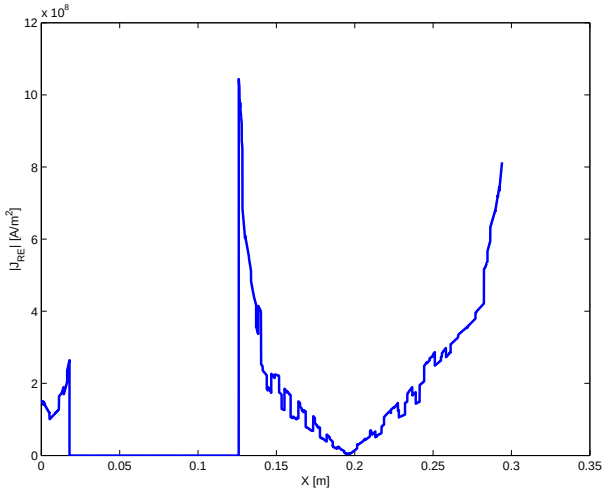

Figure 11. The absolute value of the real part of induced current density along the line (TEAM problem 7 geometry).

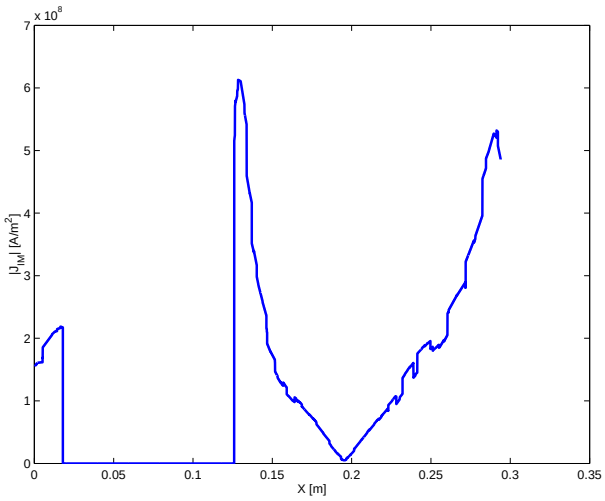

Figure 12. The absolute value of the imaginary part of induced current density along the line (TEAM problem 7 geometry).